Title

Arsenic hyperaccumulator Pteris vittata shows reduced biomass in soils with high arsenic and low nutrient availability, leading to increased arsenic leaching from soil

Authors

Matzen, SL
Lobo, GP
Fakra, SC
et al.

Publication Date

2022-04-01

DOI

10.1016/j.scitotenv.2021.151803

Science of the Total Environment 818 (2022) 151803

Contents lists available at ScienceDirect

Science of the Total Environment

journal homepage: www.elsevier.com/locate/scitotenv

Arsenic hyperaccumulator *Pteris vittata* shows reduced biomass in soils with high arsenic and low nutrient availability, leading to increased arsenic leaching from soil

S.L. Matzen [a,1], G.P. Lobo [b], S.C. Fakra [c], A. Kakouridis [a,2], P.S. Nico [d], C.E. Pallud [a,*]

[a] *Department of Environmental Science, Policy, and Management, University of California-Berkeley, 130 Mulford Hall, Berkeley, CA 94720, USA*
[b] *Civil and Environmental Engineering, University of California-Berkeley, 410 O'Brien Hall, Berkeley, CA 94720, USA*
[c] *Advanced Light Source, Lawrence Berkeley National Laboratory, Berkeley, CA 94720, USA*
[d] *Earth and Environmental Sciences Area, Lawrence Berkeley National Laboratory, Berkeley, CA 94720, USA*

HIGHLIGHTS

- Soil characteristics, fern growth, and transpiration affect soil arsenic leaching.
- Arsenic is more phytoavailable and leachable in soil with lower clay content.
- Stress of phytoavailable arsenic tolerance and poor nutrition limit biomass.
- Healthy fern growth enhances arsenic availability for uptake and leaching.
- Transpiration limits arsenic leaching.

GRAPHICAL ABSTRACT

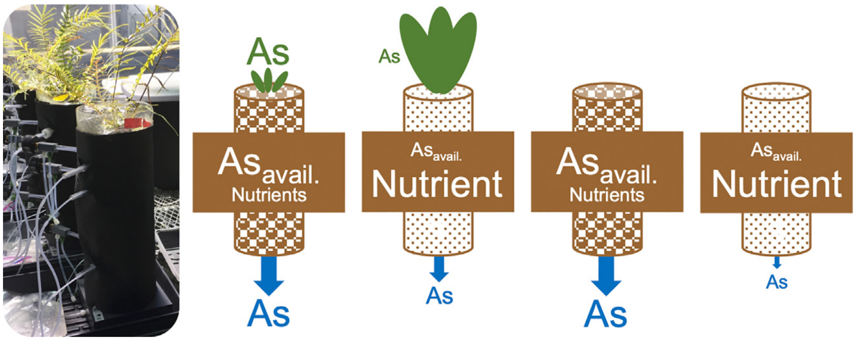

ARTICLE INFO

Article history:
Received 19 August 2021
Received in revised form 6 November 2021
Accepted 15 November 2021
Available online 20 November 2021

Editor: Filip M.G. Tack

Keywords:
Phytoextraction
Rhizosphere
X-ray fluorescence
X-ray absorption spectroscopy
Arsenic speciation
Soil texture
Unsaturated soil columns

ABSTRACT

Plant-soil interactions affect arsenic and nutrient availability in arsenic-contaminated soils, with implications for arsenic uptake and tolerance in plants, and leaching from soil. In 22-week column experiments, we grew the arsenic hyperaccumulating fern *Pteris vittata* in a coarse- and a medium-textured soil to determine the effects of phosphorus fertilization and mycorrhizal fungi inoculation on *P. vittata* arsenic uptake and arsenic leaching. We investigated soil arsenic speciation using synchrotron-based spectromicroscopy. Greater soil arsenic availability and lower nutrient content in the coarse-textured soil were associated with greater fern arsenic uptake, lower biomass (apparently a metabolic cost of tolerance), and arsenic leaching from soil, due to lower transpiration. *P. vittata* hyperaccumulated arsenic from coarse- but not medium-textured soil. Mass of plant-accumulated arsenic was 1.2 to 2.4 times greater, but aboveground biomass was 74% smaller, in ferns growing in coarse-textured soil. In the presence of ferns, mean arsenic loss by leaching was 195% greater from coarse- compared to the medium-textured soil, and lower across both soils compared to the absence of ferns. In the medium-textured soil arsenic concentrations in leachate were higher in the presence of ferns. Fern arsenic uptake was always greater than loss by leaching. Most arsenic (>66%) accumulated in *P. vittata* appeared of rhizosphere origin. In the medium-textured soil with more clay and higher nutrient content, successful iron scavenging increased arsenic release from soil for leaching, but transpiration curtailed leaching.

---

[*] Corresponding author.
E-mail address: cpallud@berkeley.edu (C.E. Pallud).
[1] Present address: Department of Soil, Water, and Climate, University of Minnesota, Room 439 Borlaug Hall, 1991 Upper Buford Circle, Saint Paul, MN 55108, USA.
[2] Present address: Lawrence Berkeley National Laboratory, 1 Cyclotron Rd, Berkeley, CA 94720, USA.

http://dx.doi.org/10.1016/j.scitotenv.2021.151803

1. Introduction

Hyperaccumulator plants, globally over 450 species (Rascio and Navari-Izzo, 2011), take up metal(loids) from soils, then translocate and store them in their aboveground biomass (Reeves, 2006). Considerable research has been done on hyperaccumulators aiming at remediating soil and water contaminated with metal(loid)s (*e.g.* phytoextraction) (Chaney et al., 2007; Li et al., 2018; Rascio and Navari-Izzo, 2011; Tack and Meers, 2010; Wu et al., 2015) and determining mechanisms of metal(loid) accumulation in aboveground biomass (Baker and Whiting, 2002; Danh et al., 2014; Rascio and Navari-Izzo, 2011; van der Ent et al., 2013; Xie et al., 2009).

Hyperaccumulator rhizosphere chemistry affects metal(loid) plant availability (Alford et al., 2010; Kidd et al., 2009; Wagner et al., 2020) and metal release from soil has been tied to nutrient scavenging (Audet, 2013; Meharg and Hartley-Whitaker, 2002). Manipulating metal(loid) solubility in soils to increase hyperaccumulator uptake and therefore phytoextraction rates is attractive (Kidd et al., 2009; Lessl and Ma, 2013; Saifullah et al., 2009; Wenzel et al., 2003; Yang et al., 2019). However, increases in metal(loid) solubility in soil could lead to metal(loid) leaching if the mobilized fraction is not completely taken up by the target plant, a potentially negative and poorly characterized outcome of phytoextraction.

Extensive work has explored arsenic phytoextraction with the fern *Pteris vittata* (Danh et al., 2014; Fayiga and Saha, 2016; Xie et al., 2009) as an *in situ* alternative to soil excavation-based arsenic remediation methods (Tack and Meers, 2010; Wan et al., 2016). The fern hyperaccumulates arsenic under a range of soil physicochemical conditions (Caille et al., 2004; Ciurli et al., 2014; da Silva et al., 2018; Kertulis-Tartar et al., 2006; Ma et al., 2001). However, phytoextraction rates are slow even at moderate concentrations (~100 mg As/kg soil), leading to estimated remediation times on the order of decades or more to deplete soil arsenic to background levels (Lessl and Ma, 2013; Niazi et al., 2012; Shelmerdine et al., 2009). Manipulations to increase soil arsenic availability, fern biomass, and fern arsenic uptake through nutrient application and mycorrhizal fungi inoculation have been investigated to increase phytoextraction rates.

In particular, complex relationships between arsenic and phosphorus availability in soil and uptake in *P. vittata* vis-à-vis fern nutrient deserve further elucidation, including the effects of soil phosphorus relative to supplemental phosphorus (Cao et al., 2003; Chen et al., 2002; da Silva et al., 2018; Fayiga and Ma, 2006; Lessl and Ma, 2013; Tu and Ma, 2003). According to the phosphorus starvation theory (Audet, 2013; Meharg and Hartley-Whitaker, 2002), arsenic uptake in *P. vittata* could be a byproduct of nutrient acquisition, especially iron and phosphorus. Phosphate and arsenate are chemical analogues found in soils associated with iron oxides (Lombi et al., 2000; Smith et al., 2006) and can be released in the rhizosphere through similar biogeochemical processes (Marschner and Romheld, 1994).

Furthermore, *P. vittata* associates with mycorrhizal fungi including *Funneliformis* (formerly *Glomus*) spp. (Leung et al., 2006; Wu et al., 2007). Like hyperaccumulators, mycorrhizal fungi evolved under phosphorus starvation conditions, can support plants under nutrient deficiency, drought, and metal stress, and have stress tolerance mechanisms that differ from and are possibly complementary to those of hyperaccumulators (Audet, 2013). Inoculation with mycorrhizal fungi could increase *P. vittata* biomass (Liu et al., 2005; Matzen et al., 2020; Trotta et al., 2006), nutrient, water, and possibly arsenic access (Karandashov and Bucher, 2005), with species adapted to local (metal-enriched) soils important in addition to generalists (Trotta et al., 2006).

Moreover, soil clay content (*i.e.*, soil texture) affects nutrient and arsenic availability (Smith et al., 2006). Clay-sized particles, the smallest of soil particles, include mineral phases such as iron oxides, aluminum oxides, and silicate clay minerals that provide a large surface area for adsorption of arsenic, phosphorus, and other nutrients (Lombi et al., 2000; Manning and Goldberg, 1996; Redman et al., 2002). Arsenic has been shown to be more plant available (Jacobs and Keeney, 2008; Woolson et al., 1973) and more leachable (Hale et al., 2008; Masscheleyn et al., 1991) in soil with lower clay content.

Few arsenic phytoextraction studies have investigated arsenic leaching during *P. vittata* growth or computed arsenic budgets. After *P. vittata* growth, similar (Yang et al., 2012) or lower (Cao et al., 2003) levels of arsenic in leachate were found compared to non-phytoextracted soils. In long-term field studies, greater arsenic depletion has been observed for soil below the fern root zone, compared to surface depths (Kertulis-Tartar et al., 2006; Matzen et al., 2020; Niazi et al., 2012), which could indicate leaching of arsenic below the root zone. It is important to quantify arsenic cycling in the *P. vittata*-soil-water system *during* growth, because *P. vittata* growth processes might lead to spatiotemporally heterogeneous arsenic leaching.

Unsaturated flow-through soil column studies with plants are a powerful setup to quantify arsenic cycling in controlled whole plant-soil-water systems that approximate natural systems. With such systems, water balances including transpiration can be calculated, and arsenic transport in soil porewater can be quantified (Zhang and Selim, 2006). Combining such soil columns studies with X-ray absorption near edge structure (XANES) spectroscopy and X-ray fluorescence (XRF) imaging at the micron scale allows us to investigate rhizosphere processes (Kopittke et al., 2017) and relate rhizosphere processes to arsenic cycling at the system scale. We conducted a 22-week soil column study with moderately contaminated soil planted with *P. vittata* to determine the effects of soil texture (a proxy for nutrient and arsenic availability), phosphorus application, and fungi inoculation on arsenic cycling in the plant-soil-water system. We used synchrotron-based spectromicroscopy to determine arsenic speciation in bulk and rhizosphere soils and propose mechanisms of arsenic mobilization for plant uptake and/or leaching. We observed greater arsenic uptake and leaching with smaller fern biomass in soil with lower clay content across all treatments, suggesting significant plant growth trade-offs associated with arsenic hyperaccumulation and phytoextraction.

2. Methods

2.1. Soils

Two soils moderately contaminated with arsenic and with contrasting textures (medium-textured soil, 55% sand, 17% silt, 28% clay, 138.0 ± 1.5 mg As/kg; coarse-textured soil, 79% sand, 0.34% silt, 20% clay, 95.3 ± 1.1 mg As/kg; Table 1) were excavated from the 0–30 cm depth in a former railroad right-of-way (Berkeley, CA, USA). Soils were sieved (4 mm) and stored field-moist at 5 °C in sealed containers under oxic conditions. Soil pH was measured on triplicate samples and cation exchange capacity and percent organic matter were measured on duplicate samples as described previously (Pallud et al., 2020). Bulk density was measured in triplicate on intact cores of a known volume from which the volume of the fraction >2 mm was subtracted, following a modified protocol for rocky soils (United States Department of Agriculture, 2001). Porosity was calculated from bulk density (Grossman and Reinsch, 2002). Soil texture was measured in triplicate with the hydrometer method (Gee and Or, 2002). In both soils, clay minerals identified with X-ray diffraction (PANalytical) following USGS protocols (Poppe et al., 2002) included nontronite, trioctahedral montmorillonite, and/or vermiculite.

2.2. Soil column study

Experiments with novel unsaturated flow-through soil columns with plants were performed in triplicate to estimate arsenic uptake by *P. vittata*, arsenic desorption and transport in soil, and arsenic leaching. We compared (i) control columns without amendments with (ii) columns fertilized with phosphorus

Table 1
Properties of soil before phytoextraction.

	Sand[a] (%)	Silt[a] (%)	Clay[a] (%)	Texture	Bulk density[a] (g/cc)
Medium	54.7 ± 0.3	17 ± 1	28 ± 1	Sandy clay loam	1.06 ± 0.02
Coarse	79.3 ± 0.5	0.3 ± 0.5	20.4 ± 0.5	Sandy clay loam	1.60 ± 0.08

	pH[b]	CEC (meq/100 g)	Organic matter (%)	Total[c] As (mg/kg)
Medium	6.00 ± 0.00	19.99 ± 0.02	5.89 ± 0.08	138 ± 2
Coarse	6.93 ± 0.06	4.64 ± 0.04	0.95 ± 0.01	95 ± 1

	Extractable (mg/kg)[d]					
	P	K	Ca	Mg	Zn	Mn
Medium	17.7 ± 0.4	288 ± 5	2591 ± 4	384.2 ± 0.7	57.4 ± 0.5	4.0 ± 0.3
Coarse	8.1 ± 0.1	56.5 ± 0.2	729 ± 9	103.6 ± 0.2	4.6 ± 0.2	4 ± 2

	Extractable (mg/kg)[d]					
	Cu	Fe	Pb	Al	Na	S
Medium	2.1 ± 0.1	7.8 ± 0.6	12.3 ± 0.2	3.7 ± 0.1	30.6 ± 0.5	23.6 ± 0.5
Coarse	1.7 ± 0.2	2.52 ± 0.03	2.16 ± 0.01	5.38 ± 0.02	13.5 ± 0.1	6.1 ± 0.4

[a] Texture and bulk density are means of 3 replicates.
[b] Mean of 3 replicates, in water.
[c] Mean and standard error of soil in each of 3 replicate columns, before soil treatments applied.
[d] Mean of 2 replicates, Modified Morgan extractable, before soil treatments applied.

(CalPhos™, 7.9% P, 18% Ca; 1.2 g P/kg soil), and (iii) columns inoculated with the fungus *F. mosseae* (INVAM; 44 mL inoculum/fern; formerly *Glomus mosseae*). Phosphorus was mixed into soil before packing columns. Fungal inoculant was applied to each hole at transplanting. Column experiments without plants ("unplanted columns") were also performed, with one replicate *per* soil *per* treatment for control and phosphorus treatments. However, because fungal inoculant was not expected to survive in the absence of ferns, unplanted column experiments with fungal inoculation were not performed. For the remainder of the manuscript, any mention of columns in text refers to planted columns, unless specifically noted.

Soil columns were made of acrylic tubes (15 cm diameter, 45 cm length). At the bottom of each column a 0.2 μm filter (contacting soil) and glass fiber filter separated soil from the effluent port, which was filled with quartz sand with glass wool on either end. To ensure reproducibility between columns, they were all packed similarly at bulk density representative of field conditions (Pallud et al., 2004). Soil was well-mixed before weighing into 20 increments of equal mass appropriate for packing into a 2 cm depth. Soil was packed to a total depth of 40 cm using a custom-made 3-pronged device to apply downward force over a small surface area (Pallud et al., 2004) to avoid formation of layers. *P. vittata* ferns with bare roots and 3–7 fronds 10–20 cm in length were planted with roots 0–10 cm deep in columns. Porewater samplers (Soilmoisture Equipment Corp.) and tensiometers (Soilmoisture Equipment Corp.) were filled with degassed synthetic rain and inserted horizontally at depth (5, 10, and 27 cm) with the tip 7.5 cm inside planted columns. Columns were covered to minimize exposure of soil to light and surface evaporation from topsoil.

A synthetic rain solution that served as column influent was made following rain composition of the field site (Whitehead and Feth, 1964) adjusted to current rainfall pH (5.33). Globally, rainfall pH ranges from 3.5 to 8.0 (Wicke et al., 2014) so pH 5.33 was considered widely applicable. The synthetic rain was kept in the dark during experiments. The influent solution was supplied by a single port at the rhizome, and was eluted with a peristaltic pump through planted columns for 22 weeks at a constant flow rate (3.52 ± 0.06 mL/h) equivalent to maximum daily rainfall (0.508 cm/day) (Western Regional Climate Center, 2000). The flow rate was chosen to approximate conditions encountered in the field, made constant to simplify experiment design, and is representative of high rainfall climates and irrigated environments. A conservative bromide (Br^-) tracer was eluted through unplanted control columns for half a pore volume and the synthetic rain was eluted for 2 pore volumes (or until columns clogged) at the same flow rate as used in the planted columns.

The column experiments were conducted in a greenhouse (mean day temperature 25.8 ± 0.1 °C, mean night temperature 17.3 ± 0.05 °C, mean relative humidity 56.5 ± 0.07%) with a 16-h photoperiod.

2.3. Soil, porewater, effluent, and fern sample collection

Porewater samples (< 60 mL) were extracted from planted columns approximately every 2 weeks using acid-washed syringes maintained at 4 °C during collection. Porewater samples were immediately filtered (0.45 μm) under anoxic conditions, subsampled for analyses, and stored at −18 °C in the dark until analysis. Planted column effluent was collected weekly into polyethylene bottles (500 mL) pre-acidified with concentrated HNO_3 (70% TM grade). After collection, effluent was adjusted to 2% HNO_3, filtered (0.45 μm), and stored (4 °C) for analysis. Unplanted column effluent was collected every 228 min using a fraction collector. After collection, samples for bromide analysis were reserved and samples for arsenic analysis were combined on a weekly basis and treated the same as the planted column effluent. Pinnae samples (1 middle pair from each frond) were collected at 11 and 21 weeks.

At the end of the experiments, all aboveground biomass was removed 2 cm above the rhizome and separated based on development of sori and tissue senescence (young = sori absent to forming, mature = sori brown but not fully distended, senescent = sori fully distended, tissue browning to fully brown). Each soil column was sliced at designated depths (0–7.5 cm, 7.5–17 cm, and 17–30 cm depth intervals). The entire rhizome was removed, though not the entire root mass. All root and soil samples (collected with clean stainless-steel tweezers and spatulas from each depth intervals) were immediately stored at 4 °C.

Aboveground biomass (hereafter, frond) was washed 3 times in deionized water to remove soil particles and dust (Matzen et al., 2020). Rhizomes and root samples for elemental analysis were washed in deionized water until clean of soil. Fronds, rhizomes, and root samples for elemental analysis were dried (55 °C) for 24 h or until constant mass was achieved. Whole root samples for microprobe and DNA sequencing (to assess success of fungal inoculation) were flash-frozen in liquid nitrogen within 6 h of harvesting and stored at −80 °C until analyses. Additional root samples were dried, processed, and maintained under anoxic conditions for X-ray absorption spectroscopy (XAS) (Arai and Dahle, 2018; Matzen et al., 2020). Soil samples were either air-dried for elemental analysis or dried, processed, and maintained under anoxic conditions for XAS.

2.4. Sample analysis

Dry plant biomass was measured on pinnae, frond, and rhizome samples. Pinnae sample biomass served as a proxy for whole plant biomass during growth. Plant tissue and soil samples were digested following a modified EPA 3050B protocol described previously (Matzen et al., 2020). Total arsenic, phosphorus, and iron concentrations of soil and fern digests were determined using inductively coupled plasma optical emission spectroscopy (ICP-OES). The detection limit was 20 μg/L for each analyte. Extractable soil nutrient concentrations (Table 1) were measured as described previously (Pallud et al., 2020).

Total arsenic concentrations in effluent and porewater samples were analyzed using either ICP-OES or, if concentrations were less than 50 μg/L, hydride-generation-ICP-OES (HG-ICP-OES; detection limit 2 μg/L) after addition of 0.8 mL of 40% KI/8% ascorbic acid to 4 mL sample and 2.7 mL 1.1 M HCl (Roberts et al., 2004). In porewater, arsenic(III) concentrations were determined using HG-ICP-OES in samples buffered at pH 5.0 through addition of 2.5 mL 0.5 M disodium citrate to 2.5 mL sample, dissolved organic carbon (DOC) concentrations were analyzed using an O-I-Analytical analyzer, and pH was determined using a Denver Instruments meter with pH/ATC Sartorius ATC combination electrode. Bromide concentrations were measured using a Dionex Ion Chromatograph with a detection limit of 2.4 mg/L.

Samples of roots with rhizospheric soil, of soil aggregates, and of bulk soil were prepared for XAS, and measurements were collected as described previously (Matzen et al., 2020). Briefly, whole roots and root or aggregate thin sections were mounted onto a Peltier cooling stage (−22 °C) for X-ray microprobe analysis, X-ray fluorescence (XRF) mapping and X-ray absorption near-edge structure (XANES), at the Advanced Light Source (ALS) XFM beamline 10.3.2 (Marcus et al., 2004), Lawrence Berkeley National Laboratory (LBNL, Berkeley, CA, USA). Bulk X-ray XANES spectra were collected at Stanford Synchrotron Radiation Laboratory (SSRL, Menlo Park, CA, USA) beamline 7.3 on bulk powdered samples mounted on filters. Least-square linear combination fitting was performed with custom LabVIEW software and XAS databases of iron and arsenic compounds available at beamline 10.3.2. Details of the spectromicroscopy measurements are available in the Supplemental Information.

2.5. Root arbuscular mycorrhizal fungi (AMF) identification

To determine whether fungal inoculation increased abundance of *F. mosseae* in inoculated plants, root DNA was extracted (Brodie et al., 2011) and sequenced. A sequencing library was prepared (Dumbrell et al., 2011; Egan et al., 2018; Lee et al., 2008), PCR was performed, and PCR products were sent to QB3-Berkeley Genomics for sequencing on the Illumina MiSeq platform. Processed sequences (Bolyen et al., 2019; Callahan et al., 2016) were clustered into OTUs at the 97% sequence similarity and taxonomy was assigned using the MaarjAM database (version 05.06.2019) (Öpik et al., 2010). Full details are available in the Supplemental Information.

2.6. Bromide breakthrough curve and arsenic transport modeling

Transport and desorption of total arsenic within the soil columns was modeled using a solute transfer model through unsaturated soil (Gaudet et al., 1977) amended with a retardation factor to account for the desorption of arsenic from soil. In unsaturated soils, the transport of solutes occurs in two phases: (1) a mobile phase where water flows through the porous medium and (2) an immobile phase in which water is stagnant within dead-end pores or between soil particles. Briefly, bromide tracer breakthrough curves collected from unplanted columns were used to constrain transport parameters and to check for non-ideal flow conditions in the columns. Adsorption constants were fit that best described the total arsenic desorption from each of the four unplanted soil columns. Changes in arsenic concentrations in the solid phase (dC_{s_m}/dC and dC_{s_im}/dC), where C_{s_m} and C_{s_im} are the arsenic concentration within the mobile and immobile solid phase (mg As/g dry soil), respectively, were derived from isotherm equations, (*e.g.* Freundlich, Langmuir or linear) (Holzbecher, 2012). Since the binding sites in the soil are non-uniform, the Freundlich isotherm was used in the model as it represents multiple types of binding sites. Full details are available in the Supplemental Information.

2.7. Fern arsenic accumulation, cumulative leaching, and mass balance calculations

The amount of arsenic accumulated *per* fern aboveground biomass (mg/frond type) or *per* rhizome (mg/rhizome) was calculated by multiplying the arsenic concentration by the dry biomass of aboveground biomass or rhizome, respectively. Volume (V) of transpired water *per* fern was calculated by subtracting effluent volume from influent volume *per* column (Eq. 1), assuming all influent not collected as effluent was transpired. This assumption overestimates transpiration in columns where soil water content increased during the flow-through study.

$$V_{transpired\ water} = V_{influent} - V_{effluent} \tag{1}$$

The mass (M) of arsenic in bulk porewater contributed *via* transpiration to the total mass of arsenic accumulated in the fern aboveground biomass was calculated by multiplying the mean arsenic concentration in porewater at 10 cm depth by the volume of transpired water *per* column (Eq. 2). The same calculation was performed for phosphorus and iron.

$$M_{As,fern,pw} = \left[As_{pw}\right] \times V_{transpired\ water} \tag{2}$$

The mass of arsenic in the fern was considered to be the sum of arsenic taken up through transpiration of bulk porewater and arsenic taken up from other sources (*e.g.*, rhizosphere porewater) (Eq. 3).

$$M_{As,fern,total} = M_{As,fern,pw} + M_{As,fern,other} \tag{3}$$

To calculate the cumulative mass of arsenic and phosphorus leached *per* column over 22 weeks, porewater and effluent volume were added together and multiplied by effluent arsenic or phosphorus concentration *per* week, assuming the porewater removed during sampling would have contributed to effluent (Eq. 4). The cumulative mass leached *per* column was then normalized to the number of days effluent flowed from the column.

$$M_{As,leached} = \sum_{n=1}^{22} \left(V_{pw} + V_{eff}\right) \times \left[As_{eff}\right]_n \tag{4}$$

Final soil arsenic concentrations were normalized to initial soil arsenic concentrations *per* column. To calculate the mass balance of arsenic at termination of the study, the masses of arsenic accumulated in the fern, retained in soil in each depth interval (0–7.5, 7.5–17, and 17–40 cm), extracted in porewater, and leached in effluent, were each normalized to initial mass of arsenic in soil and then summed (Eq. 5). Mass of arsenic in roots was not included, as root mass was not measured, and concentrations of arsenic in roots were much lower than in aboveground biomass. If all arsenic was accounted for, the mass balance was expected to equal approximately 100%.

$$Mass\ balance = \left[\left(As_{fronds} + As_{rhiz} + As_{pw} + As_{soil,0-7.5cm} + As_{soil,7.5-17cm} + As_{soil,17-40cm} + As_{leached}\right)/As_{init}\right] \times 100 \tag{5}$$

2.8. Statistical analysis

Statistical analysis was performed in R (R Core Team, 2020). Analyses of covariance were performed on linear models to analyze main effects of explanatory variables including time (continuous), depth (continuous), soil, and treatment on response variables including fern arsenic concentrations, biomass, arsenic accumulation, arsenic uptake rate, and changes in soil arsenic concentrations during phytoextraction. Models were selected based on AIC criteria using the MuMIn package (Barton, 2019). Two-way interactions were included when those models were most highly ranked. Regression summaries were used to compare effects of explanatory variables, and differences in means were determined with Tukey's Honestly Significant Difference test on means normalized to initial soil arsenic concentration where appropriate. A paired *t*-test was used to determine the mass balance across all columns, comparing mass arsenic leached *per* column to mass arsenic accumulated *per* fern. Effects of soil and treatment on the AMF assemblage were determined using a permutational multivariate analysis of variance (Oksanen et al., 2020) with pairwise comparisons.

3. Results

3.1. *P. vittata* arsenic and nutrient uptake

Pinnae arsenic concentrations differed dramatically with soil type ($P < 0.001$). For the coarse-textured soil, arsenic concentrations in sampled pinnae ranged up to 1890 mg/kg after 11 weeks and increased ($P < 0.001$) 2–3-fold after 21 weeks (Fig. 1A). Pinnae arsenic concentrations were considerably lower ($P < 0.001$) for the medium-textured soil, never reaching the hyperaccumulation threshold (1000 mg/kg) (Fig. 1A). The interaction of soil by time ($P < 0.001$) indicated that pinnae arsenic concentrations were lower at 21 weeks in ferns growing in the medium-textured soil compared to coarse-textured soil. The mass of arsenic accumulated in sampled pinnae increased ($P < 0.001$) over time, increasing 4–5 times up to 1.1 mg at 21 weeks in the coarse-textured soil and 2–3 times up to 0.67 mg at 21 weeks in the medium-textured soil (Fig. 1B).

At final harvest, soil type similarly affected fern frond arsenic concentrations ($P < 0.001$) and mass of accumulated arsenic *per* fern ($P < 0.01$) yet had the reverse effect on whole plant biomass ($P < 0.001$) (Fig. 2A-C). Fern arsenic concentrations in coarse-textured soil ferns ranged between 2666 and 3570 mg/kg for the whole plant, up to 10 times higher ($P < 0.001$) than the values in medium-textured soil ferns. The total mass of accumulated arsenic in coarse-textured soil ferns ranged from 15.2 to 20.2 mg/fern, about two times higher ($P < 0.01$) than in the medium-textured soil (Fig. 2B). However, the fern dry biomass was 3–4 times higher ($P < 0.001$) in the medium-textured soil than in the coarse-textured soil, with values between 20.1 and 23.5 g for the whole plant (Fig. 2C). Soil treatment did not affect whole plant arsenic concentrations ($P = 0.34$), mass of accumulated arsenic ($P = 0.82$), or biomass ($P = 0.32$).

Arsenic concentrations were greater ($P < 0.001$) by up to 2 orders of magnitude in fern aboveground biomass compared to the rhizome and roots (Fig. 2A). Mass of accumulated arsenic was greater ($P < 0.001$) by an order of magnitude in aboveground biomass compared to rhizomes (Fig. 2B). Interactions of plant part biomass by soil ($P < 0.001$) and by treatment ($P < 0.05$) showed that senescent fronds were larger in the medium-textured soil ferns compared to coarse-textured soil ferns, yet were smaller in phosphorus-treated ferns across both soils compared to in other treatments.

Within aboveground biomass alone, arsenic concentrations were up to 8 times lower in mature ($P < 0.05$) and senescent ($P < 0.001$) fronds, compared to young fronds. However, total mass of accumulated arsenic was

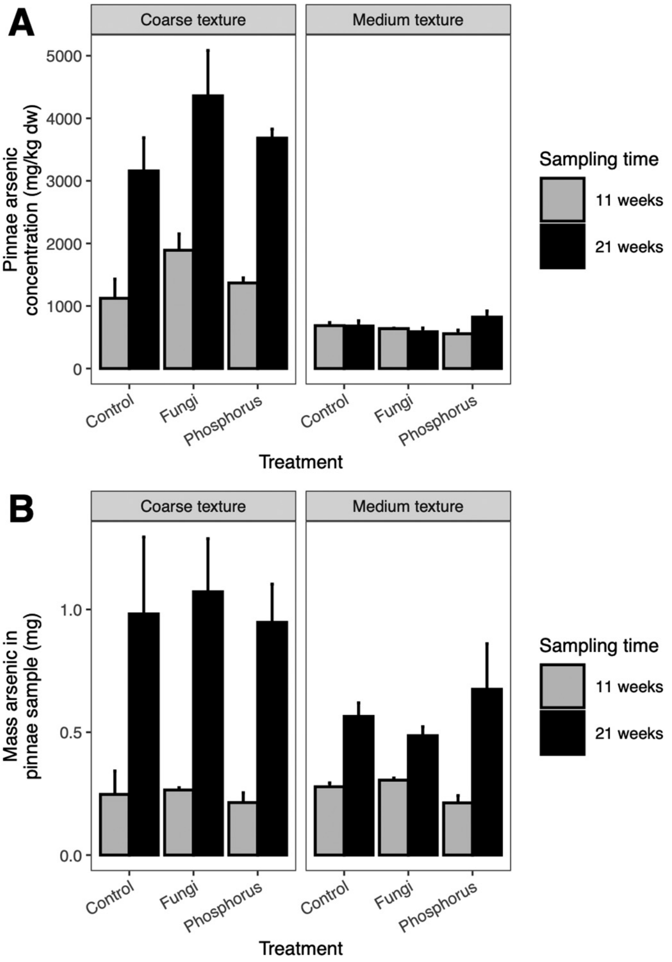

Fig. 1. Effect of soil inoculation with fungi (*F. mosseae*) and of fertilization with phosphorus on (A) arsenic concentrations and (B) mass of arsenic accumulated in pinnae at 11 (grey) and 21 (black) weeks of growth, in coarse- (left panels) and medium-textured (right panels) soils. Bars represent the mean while error bars represent standard error of 2–3 replicates.

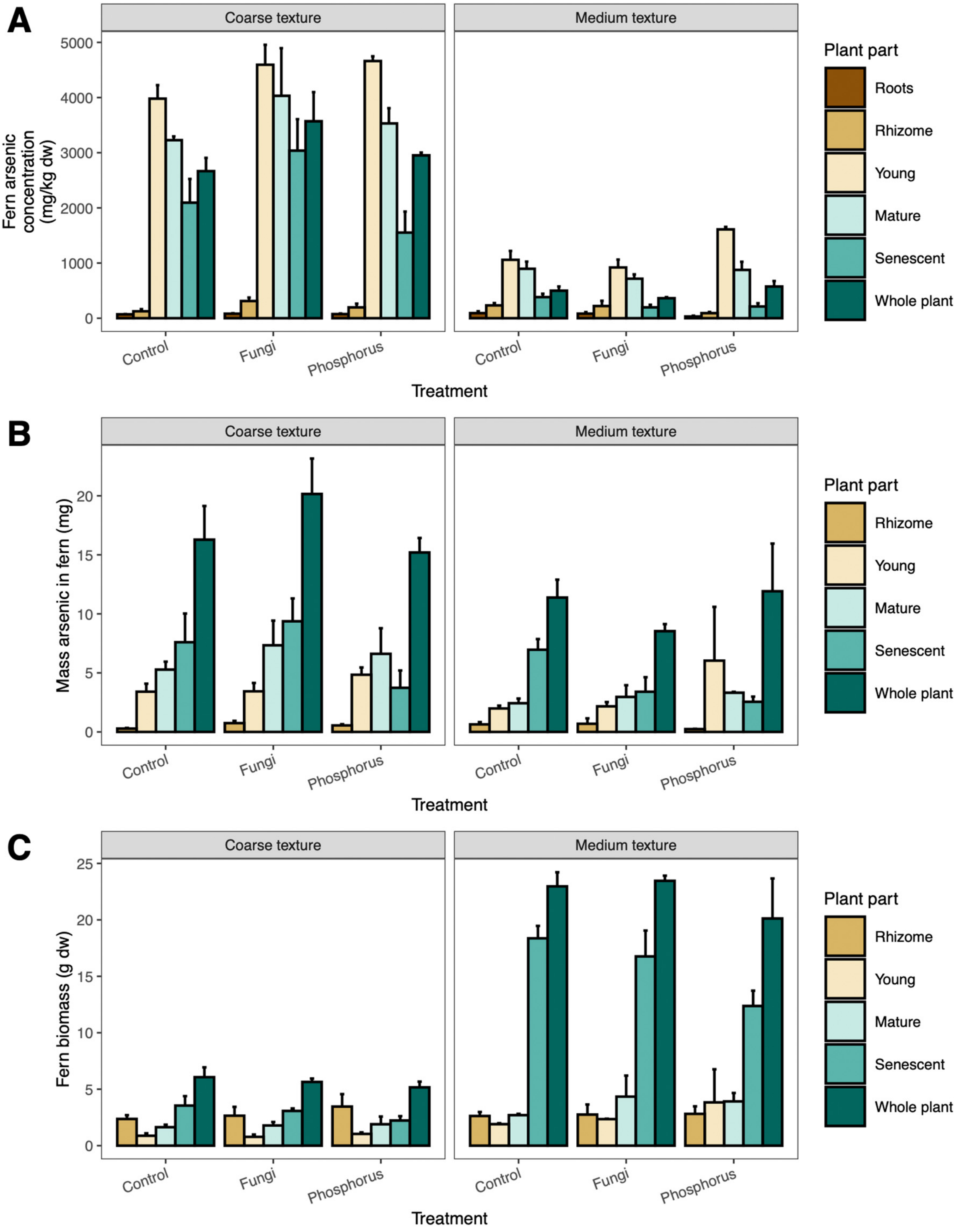

Fig. 2. Effect of soil inoculation with fungi (*F. mosseae*) and of fertilization with phosphorus on (A) arsenic concentrations, (B) dry fern aboveground biomass and (C) mass of arsenic accumulated in fern roots ((A) only), rhizomes, young fronds, mature fronds, senescent fronds, and the whole plant at final harvest at 22 weeks of growth, in coarse- (left panels) and medium-textured (right panels) soils. Bars represent the mean while error bars represent standard error of 2–3 replicates.

greater ($P < 0.05$) in senesced fronds (2.6 to 9.4 mg As/senescent fronds), compared to young fronds (2.0 to 6.0 mg As/young fronds) across both soils. Here, the interaction of frond age and treatment ($P < 0.05$) indicated phosphorus-treated senesced fronds accumulated less total arsenic than young fronds.

Whole plant phosphorus concentrations were 20% lower ($P < 0.05$) in ferns grown in the medium-textured soil (mean 1814 mg/kg), compared to in the coarse-textured soil (Fig. SI-3A). In contrast, mean iron concentrations were two to six times higher ($P < 0.05$) in ferns grown in the medium-textured soil (means 125 to 435 mg/kg), compared to in the coarse-textured soil (Fig. SI-3B). Phosphorus concentrations were higher in phosphorus-treated ferns ($P < 0.05$).

3.2. Bulk soil arsenic concentrations

Across soils, soil arsenic concentrations decreased ($P < 0.001$) by up to 25% over the experiment period (Fig. SI-4). Across soils, final concentrations in the surface 0–7.5 cm depth interval were 75 to 91% of initial concentrations, which was lower (P < 0.001) compared to the 7.5–17 cm and 17–40 cm depth intervals, where concentrations were 85 to 104% of initial values. In the coarse-textured soil only, no significant differences were found within a treatment or depth. In the medium-textured soil only, final soil arsenic concentrations increased with depth (P < 0.001) and were lower (P < 0.001) in *F. mosseae*-inoculated and phosphorus-treated soil compared to the control.

3.3. Porewater elemental concentrations

Across soils, soil (*P* < 0.001), time (P < 0.001), and depth (P < 0.001) affected porewater total arsenic concentrations (Fig. 3A-B). In the coarse-textured soil, arsenic concentrations decreased after 3 to 7 weeks, with concentrations higher in the 27 cm depth than surface depths for the remainder of the experiments. In the medium-textured soil, porewater could be

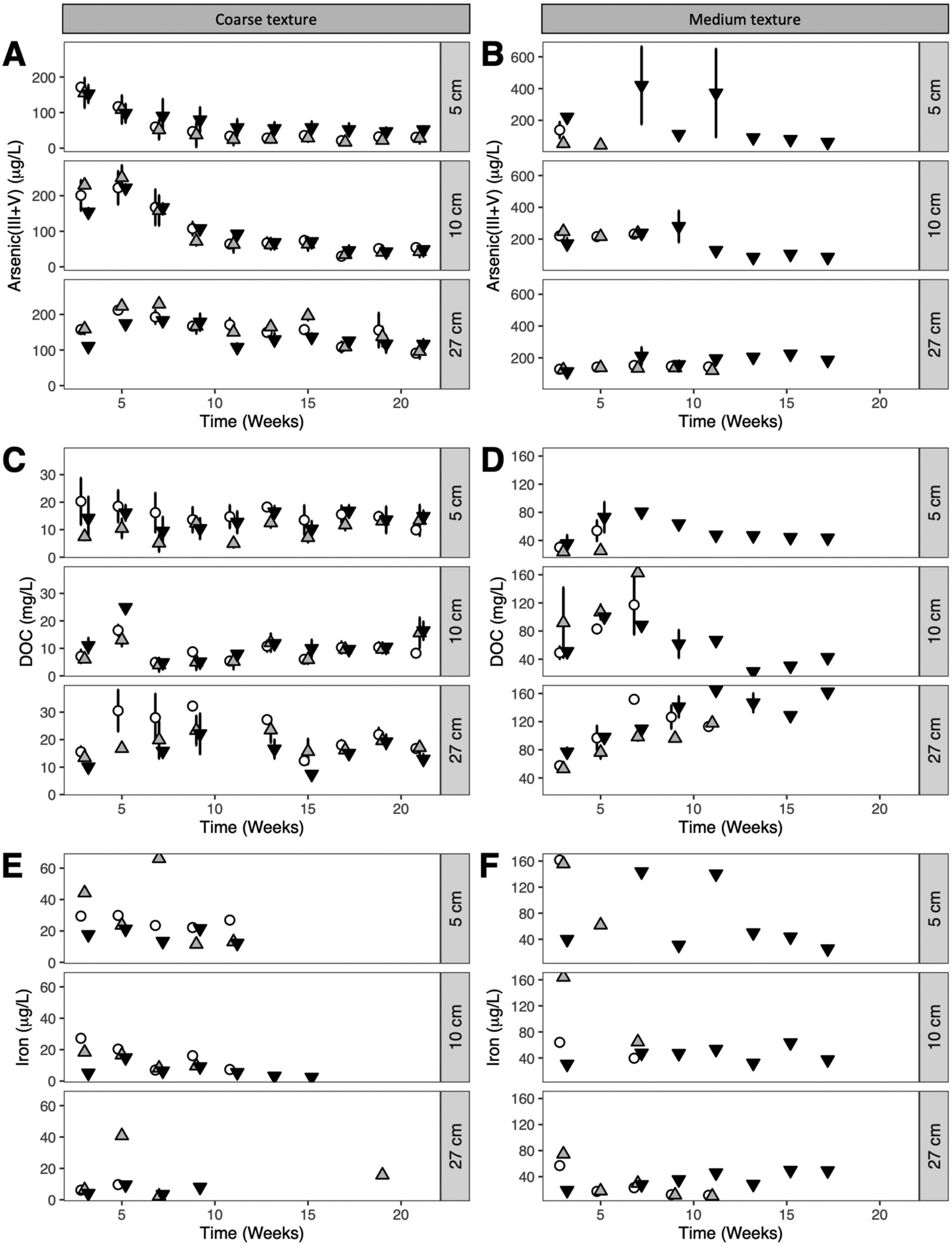

Fig. 3. Porewater concentrations of (A-B) arsenic(III + V), (C-D) dissolved organic carbon (DOC), and (E-F) iron in experiments with coarse- (left panels) or medium-textured soil (right panels). Open circles represent control columns, while grey triangles represent columns inoculated with fungi (*F. mosseae*), and black triangles represent columns fertilized with phosphorus. Note the different y-axis scales. Points represent mean and standard error of porewater extracted from 2 to 3 replicates columns. In some cases, porewater could not be extracted from columns.

extracted from the phosphorus-treated columns till 17 weeks, longer than the control and *F. mosseae*-inoculated columns, where porewater extraction was not possible as early as 5 weeks into the study. Interactions of soil and time ($P < 0.001$), soil and depth ($P < 0.001$), and soil and treatment ($P < 0.01$) showed that in the medium-textured soil, porewater arsenic concentrations slightly increased with time, decreased with depth, and increased with phosphorus treatment. Arsenic(III) concentrations were very low in the coarse-textured soil porewater, less than 4.4 μg/L, but were higher ($P < 0.001$) in the medium-textured soil, with a mean of 13.6 μg/L increasing up to a peak of 109 μg/L in weeks 5 to 9 in the phosphorus treated columns (Fig. SI-5A-B).

Concentrations of DOC were less than 32 mg/L in the coarse-textured soil porewater but higher ($P < 0.001$) in the medium-textured soil porewater, where they reached 165 mg/L (Fig. 3C-D). Depth affected ($P < 0.001$) porewater DOC concentrations. Interactions of soil by week ($P < 0.001$) and soil by depth ($P < 0.001$) showed that DOC concentrations increased with time and depth in the medium-textured soil but not coarse-textured soil.

Porewater iron concentrations were less than 66 μg/L in the coarse-textured soil but higher ($P < 0.001$) in the medium-textured soil, up to 164 μg/L, and decreased with time ($P < 0.001$) (Fig. 3E-F). A significant soil by depth ($P < 0.001$) interaction showed that iron concentrations decreased with depth in the medium-textured soil porewater.

Phosphorus concentrations were less than 0.60 mg/L in the coarse-textured soil porewater but were higher ($P < 0.001$), up to 3 times those values, in the medium-textured soil porewater, and decreased ($P < 0.001$) with time in both soils (Fig. SI-5C-D). Phosphorus and total arsenic concentrations were moderately correlated ($R^2 = 0.41$).

Soil ($P < 0.001$), time ($P < 0.001$), depth ($P < 0.001$), and treatment ($P < 0.001$) affected porewater pH, which ranged from 6.0 to 8.9 in both soils and increased significantly with depth across both soils (Fig. SI-5E-F). Interactions of soil by time ($P < 0.001$), by depth ($P < 0.001$), and by treatment ($P < 0.01$) showed in the medium-textured soil that pH increased over time, decreased with depth, and increased with phosphorus treatment.

3.4. Effluent elemental concentrations, volume, and cumulative leaching

A soil by presence/absence of ferns interaction indicated that effluent arsenic concentrations were higher in the presence of ferns in the medium-textured soil ($P < 0.001$), but that presence of ferns did not affect effluent arsenic concentrations in the coarse-textured soil (Fig. 4A).

Across both soils, effluent arsenic concentrations increased with time ($P < 0.001$) (Fig. 4A). Effluent arsenic concentrations were lower ($P < 0.001$) in the medium-textured soil (range 43.0–152.9 μg/L) than in the coarse-textured soil (range 94.0–241.0 μg/L). Phosphorus treatment lowered arsenic concentrations in effluent of both soils ($P < 0.01$), regardless of whether ferns were present.

Effluent volume ($P < 0.001$) and cumulative arsenic loss ($P < 0.001$) were greater in the absence of ferns, with up to 67 mL/day effluent leading to cumulative arsenic loss of up to 12.6 μg/day by leaching (Fig. 4B-C).

Regardless of whether ferns were present, effluent volumes were greater in the coarse-textured soil ($P < 0.001$) (Fig. 4B-C) where effluent

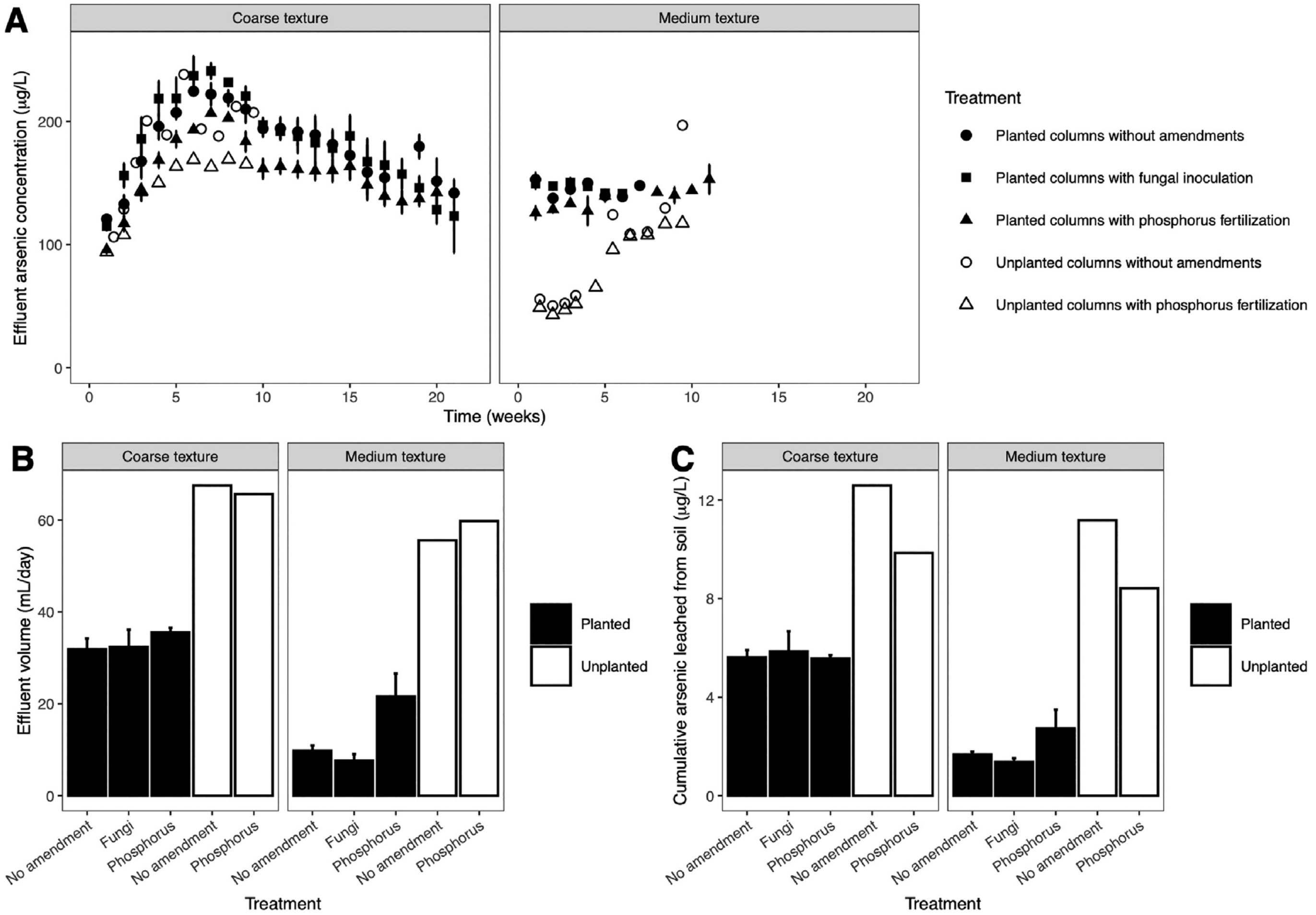

Fig. 4. (A) Arsenic concentrations in column effluent over 22 weeks of *P. vittata* growth (closed shapes; planted columns) or over 10 weeks in the absence of *P. vittata* (open shapes; unplanted columns), (B) effluent volume from planted and unplanted columns, and (C) cumulative arsenic leached from soil in planted and unplanted columns. Columns were filled with coarse- (left panels) or medium-textured (right panels) soil. Points/bars represent mean and standard error of 2–3 replicates (planted columns) or data of 1 replicate (unplanted columns).

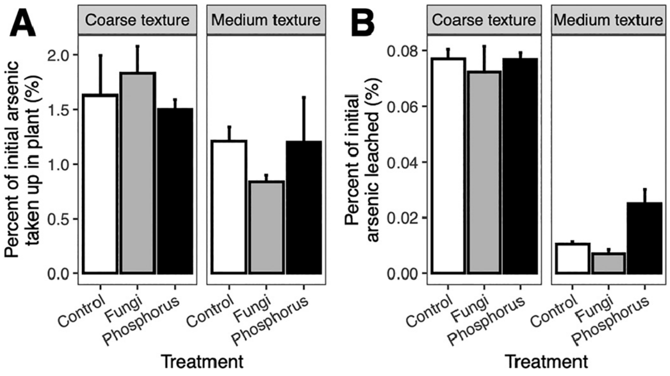

Fig. 5. (A) Percent of the arsenic initially present in planted soil columns accumulated in ferns, and (B) percent of the arsenic initially present in planted soil columns leached, after 22 weeks of *P. vittata* growth. Columns were filled with coarse- (left panels) or medium-textured (right panels) soil. Points/bars represent mean and standard error of 2–3 replicates.

flow lasted 22 weeks in the presence of ferns (Fig. 4A), leading to cumulative arsenic loss of up to 5.9 μg/day by leaching. This cumulative arsenic loss was more ($P < 0.001$) than from the medium-textured soil in the presence of ferns, where effluent flow ceased at 7 weeks (Fig. 4A) with 50% less loss by leaching. Although in the presence of ferns effluent volumes were greater in phosphorus-treated columns ($P < 0.05$), this did not lead to greater cumulative loss of arsenic from phosphorus-treated soil ($P = 0.409$). In the absence of ferns, cumulative arsenic lost from soil was lower in the phosphorus-treated soil ($P < 0.01$).

3.5. Mass balance

Across all soils and treatments, a mean of 90.7% (79.9 to 101.2%) of initial arsenic was recovered in final soil, plant tissue, porewater samples, and effluent (data not shown). Approximately 1.5 to 1.8% of the initial arsenic present in soil was accumulated in ferns growing in the coarse-textured soil, more ($P < 0.001$) than in the medium-textured soil, where only 0.8 to 1.2% of the initial arsenic was accumulated (Fig. 5A). In both soils, the percent of initial soil arsenic taken up into plants exceeded ($P < 0.001$) the percent of initial arsenic leached (Fig. 5B). About 0.07% of initial arsenic was lost to leaching from the coarse-textured soil, but less than 0.025% was lost from the medium-textured soil.

In the coarse-textured soil, a smaller mass of arsenic ($P < 0.001$) (Table 2) in bulk porewater was contributed *via* transpiration to the mass of arsenic accumulated in the fern aboveground biomass, compared to the medium-textured soil. Only 4 to 5% of arsenic in coarse-textured soil ferns was contributed from transpiration flux of bulk porewater, compared to 17 to 34% of arsenic in medium-textured soil ferns (Table 2). Similar trends were found for phosphorus ($P < 0.001$) and iron ($P < 0.01$) (data not shown).

3.6. Inert tracer breakthrough curve and arsenic transport modeling

Hydrodynamic model parameters (Table SI-2) based on bromide breakthrough curves (Fig. SI-2) fit coarse-textured soil ($R^2 = 0.86–0.92$) better than the medium-textured soil ($R^2 = 0.63–0.74$). The modeled saturated fraction of soil (f) was higher in the medium- than coarse-textured soil ($f = 0.87–0.90$, medium; 0.15–0.20, coarse), as was the apparent dispersion coefficient (D_{ap}) ($D_{ap} = 0.25–0.28$, medium; 0.17–0.19, coarse). Similarly, arsenic desorption models (Table SI-2) fit the coarse-textured ($R^2 = 0.87–0.95$) soil better than the medium ($R^2 = 0.72–0.83$). The medium-textured soil had higher arsenic adsorption constants ($k = 2.1–2.9$) than the coarse-textured soil ($k = 0.5–0.9$) while arsenic desorption was linear ($n \sim 1–1.1$) from both soils over 10 weeks.

3.7. X-ray absorption near-edge structure (XANES) spectroscopy

Bulk arsenic K-edge XANES spectra of the coarse-textured soil samples indicated greater abundance of arsenic(III) in rhizosphere soil, compared to whole roots or bulk soil (Table SI-3). In contrast, in medium-textured soils, bulk spectroscopy showed rhizosphere soil arsenic(III) fractions lesser than or equal to those in roots, with even lower abundance in bulk soil (Table SI-3). In both soils, a similar or higher fraction of arsenic(III) was found in phosphorus-treated soils compared to control samples (Table SI-3).

Micro-focused arsenic K-edge XANES spectra from coarse- (Fig. 6, Fig. SI-7, Table SI-4) and medium-textured soil (Fig. SI-6, Fig. SI-7, Table SI-5) showed that across all sample types, a higher fraction of arsenic(III) was present in medium- than coarse-textured soil (Fig. SI-7). In both textures we found very little evidence of arsenic reduction (<10% As(III)) in aggregates from control soil (Fig. 6C and Fig. SI-6C, Table SI-4 and SI-5). Compared to control aggregates, a higher fraction of arsenic(III) was found in aggregates of phosphorus-treated soil in coarse- (13.4% As(III), Fig. 6C, Table SI-4) and medium- (up to 68.7% As(III), Fig. SI-6C, Table SI-5) textured soil. Similarly, in medium-textured rhizosphere soil, μXANES spectra showed a lower fraction of arsenic(III) (<10%) in control soils, but a higher fraction (up to 44.5%) in phosphorus-treated soil (Fig. SI-6B; Table SI-5).

In coarse-textured soil, the fraction of arsenic(III) on/within whole roots ranged up to 28.5% on control roots, 80.9% on *F. mosseae*-inoculated roots, and 20.0% on phosphorus-treated roots (Fig. 6A, Table SI-4). In the medium-textured soil, the fraction of arsenic(III) on/within whole roots ranged up to 99.8% on control roots, 106.0% on *F. mosseae*-inoculated roots, and at least 13.8% on phosphorus-treated roots (in some cases peak positions indicated higher fractions of arsenic(III), but good fits could not be obtained). In contrast, on particles adjacent to roots in medium-textured soil the fraction of arsenic(III) was only 18.2% in control soil and 3.5% in *F. mosseae*-inoculated soil (Fig. SI-6A, Table SI-5).

Bulk iron K-edge XANES spectra indicated iron(III) oxyhydroxides were the most abundant species (55.8 to 77.2%) in coarse textured bulk soil, rhizosphere soil, and roots (Table SI-6). In medium-textured bulk soil, rhizosphere soil, and roots, iron(III) oxyhydroxides were less abundant (38 to 44.1%) and were not present at all in phosphorus-fertilized roots (Table SI-6). Other mineral groups identified through bulk and iron K-edge μXANES spectra in both coarse- and medium-textured soil included iron(II) silicates, iron(II-III) silicates, and iron(III) silicates (Fig. SI-8, Table SI-6).

3.8. Root AMF identification

Eleven AMF operational taxonomic units (OTUs) were identified in fern roots, including *Glomus* spp. Soil texture predicted AMF community

Table 2
Mass and percent of arsenic in fern aboveground biomass contributed either from uptake of bulk porewater *via* transpiration flux, or from other sources, over 22 weeks of *P. vittata* growth in coarse- or medium-textured soil.

Treatment	Arsenic from porewater				Arsenic from other sources			
	Coarse		Medium		Coarse		Medium	
	(mg)	(%)	(mg)	(%)	(mg)	(%)	(mg)	(%)
Control	0.86 ± 0.15	5.29	2.75 ± 0.12	24.16	15.42 ± 2.98	94.71	8.63 ± 1.53	75.84
Fungi	0.82 ± 0.16	4.08	2.89 ± 0.09	33.84	19.33 ± 3.11	95.92	5.65 ± 0.51	66.16
Phosphorus	0.76 ± 0.04	5.03	2.07 ± 0.15	17.41	14.43 ± 1.25	94.97	9.84 ± 4.19	82.59

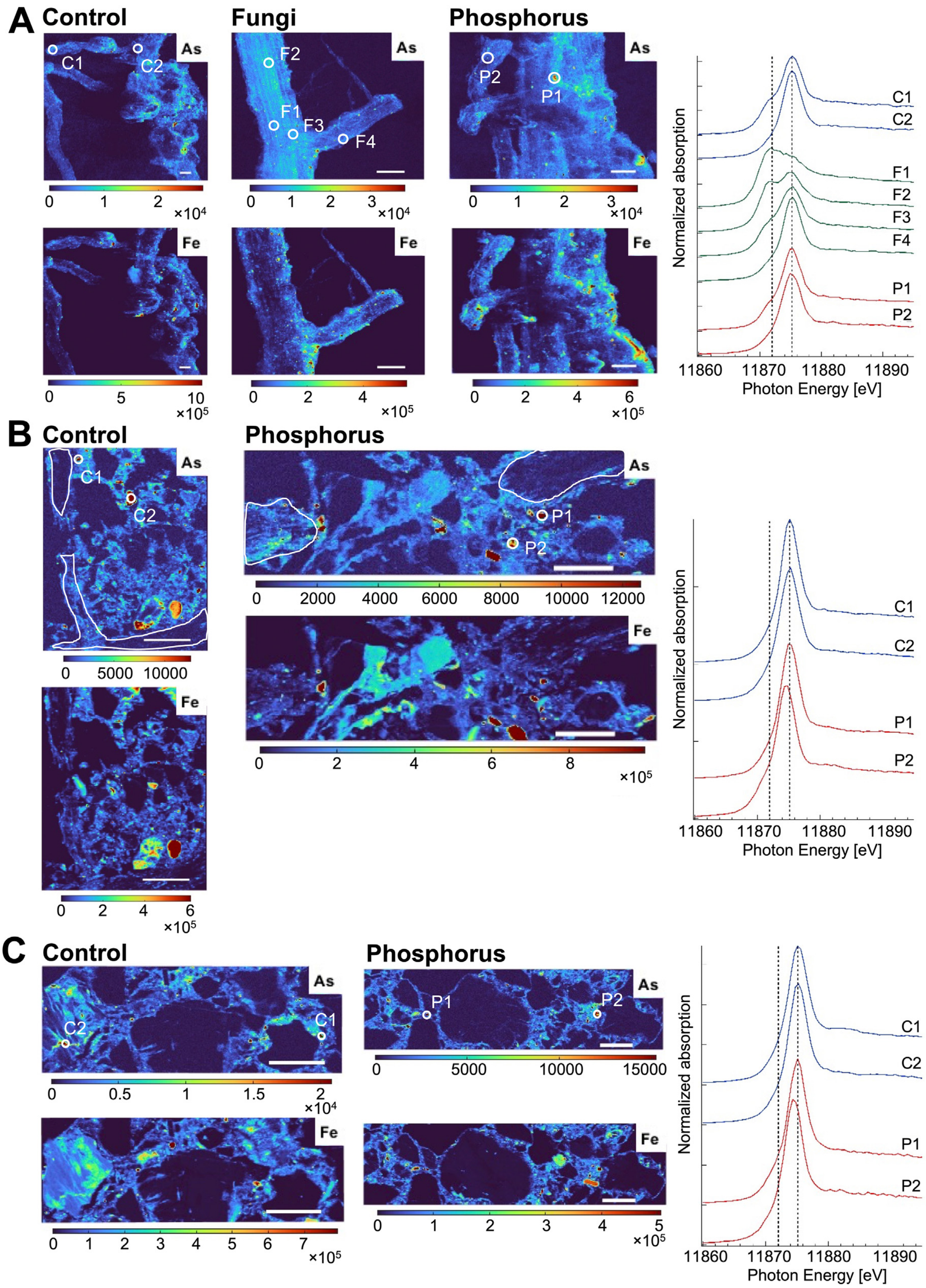

Fig. 6. Micro-focused X-ray fluorescence distribution maps of arsenic and iron in coarse-textured soil (A) whole roots with rhizospheric soil, (B) longitudinal thin sectioned roots with rhizospheric soil, and (C) thin sectioned soil aggregates. Roots (outlined in white as needed for clarity) and soil were sampled from ferns growing in coarse-textured soil. Soil treatments are indicated above image labels. Scale bars are 500 μm. In aggregate panels (C), the edge of each aggregate is at the right margin and the aggregate cross-section center is near the left margin. For each panel, selected arsenic K-edge μXANES spectra collected on spots labeled in maps are shown. Spectra were collected from 11,765 to 12,175 eV. Vertical lines denote energies of 11,872 and 11,875 eV to identify arsenic(III) and arsenic(V), respectively. Equivalent data for ferns grown in the medium-textured soil, along with the complete library of standards and LSQ fitting and valence state classification of these data, is available in the Supplemental Information.

abundance ($P < 0.001$, Fig. SI-1, Table SI-1) more strongly than did soil treatment ($P < 0.05$). Species colonizing ferns inoculated with *F. mosseae* did not differ from those identified in control or phosphorus-treated ferns.

4. Discussion

4.1. Tolerance of available arsenic exerts biomass cost

The large increase in frond arsenic concentrations we observed with increasing soil particle size suggests changes in soil texture have a strong effect on arsenic phytoextraction rates, directly through arsenic phytoavailability and/or indirectly through nutrient content and availability. Because arsenic strongly associates with the clay particle size fraction including iron oxides (Lombi et al., 2000; Smith et al., 2006), arsenic phytoavailability is lower in soils with higher clay contents (Jacobs and Keeney, 2008; Woolson et al., 1973). Our findings build on previous work showing *P. vittata* frond arsenic concentrations decrease as clay content increases in medium to fine-textured soils (Liao et al., 2004) and across wider clay content intervals (*e.g.*, 10 to 59%) (Xu et al., 2010).

Even in the presence of apparently highly plant-available arsenic, *P. vittata* did not use the rhizome as a secondary storage organ, in contrast to previous observations (Liao et al., 2004). We showed that under high phytoavailability conditions, arsenic tolerance and hyperaccumulation are simultaneous functional traits in *P. vittata*, if genetically independent (Maestri et al., 2010).

However, effective hyperaccumulation—and/or tolerance—appears to exact a metabolic cost. We found lower biomass coupled with higher arsenic concentrations in ferns growing in the coarse-textured soil, which suggests that at higher levels of phytoavailable arsenic (between that in medium-textured soil and coarse-textured soil), biomass decreases as resources are allocated to tolerance and hyperaccumulation mechanisms. In arsenic hyperaccumulation, energy is used for active transport of arsenic *via* phosphate transporters, glutathione production, arsenic reduction, transport within xylem, and sequestration (Danh et al., 2014; Maestri et al., 2010; Meharg and Hartley-Whitaker, 2002).

The lower fern biomass could also be a response to the lower nutrient content in the coarse textured soil. Like arsenic, nutrient retention can be greater in soils with higher clay and organic matter contents (Foster, 1981). Extensive nutrient scavenging in the lower-nutrient coarse textured soil could expend metabolic energy, release arsenic from soil, and increase plant uptake of arsenic, requiring more resource allocation away from biomass production toward sequestration.

4.2. Greater arsenic availability leads to leaching despite hyperaccumulation

The greater fern arsenic accumulation coupled to greater loss of arsenic by leaching observed in the coarse- compared to the medium-textured soil suggests that plant-available arsenic is also available to leach. In the coarse-textured soil, characterized by a lower iron content and adsorption capacity, arsenic appeared to leach from soil at all depths, not resorb to soil, and accumulate in porewater, leading to higher effluent arsenic concentrations. The peak in effluent arsenic concentrations in the coarse-textured soil suggests rapid, linear leaching of the most available arsenic fraction, similarly to what was observed in soils with 8% clay (Beesley et al., 2010), followed by a decrease in concentrations as the most available arsenic fractions are depleted.

Moreover, we attribute the greater effluent flow rates and duration in the coarse-textured soil to lower transpiration from the smaller aboveground fern biomass. Lower biomass leads to lower transpiration, greater infiltration, and greater leaching of available arsenic, compared to the medium-textured soil which better supported plant growth.

Yet even though the most leachable fraction was depleted early on from the coarse-textured soil, the highest fern arsenic concentrations were found in young fronds produced later in the study. This could suggest that arsenic continued to be plant available even after leaching decreased. Even in a soil with low adsorption capacity, the pools of arsenic available for leaching and plant uptake are overlapping but not identical.

4.3. Lower arsenic availability and larger ferns limit leaching

The lower arsenic leaching observed in the medium-textured soil is consistent with the greater clay and iron content and adsorption capacity, lower leachate volume, and more diffusive transport in this soil. Arsenic sorption and desorption processes appeared to occur at all depths, leading to constant porewater arsenic concentrations with depth, stable effluent arsenic concentrations lower than in the coarse-textured soil, and soil arsenic concentrations that increased with depth, indicating retention of arsenic released from the surface depth (0–7.5 cm). Nonetheless, porewater and effluent concentrations in our study were still 4 to 40 times higher than in soils with similar or higher clay content (17 to 29%) (Matzen et al., 2020; Yang et al., 2012), likely due to influent water pH and application rate simulating maximum daily rainfall conditions for an extended period.

Crucially, fast initial fern growth (indicated by higher senescent frond biomass) in the medium-textured soil, likely due to higher nutrient content and/or lower arsenic phytoavailability, led to a decrease in effluent flow and therefore arsenic leaching, as transpiration (applied water *minus* effluent) exceeded water application. In this soil, the fern required less energy to acquire nutrients, released less arsenic from soil *via* nutrient scavenging, and produced greater biomass such that arsenic concentrations in biomass were lower. The increase in mass of arsenic accumulated from 11 to 21 weeks, coupled with lower final biomass of mature and young compared to senescent fronds, shows that arsenic accumulation continued even as growth slowed. This arsenic accumulation could be due to increased nutrient scavenging associated with drought stress.

4.4. Fern growth enhances arsenic availability for uptake and leaching

The increase in arsenic concentrations in leachate in the presence of ferns growing in the medium-textured soil reveals the importance of rhizosphere processes to arsenic release for uptake and leaching. We found that arsenic depletion from the medium-textured soil was the greatest in surface soil where *P. vittata* roots are primarily located (Liao et al., 2004). Moreover, in both soils we calculated that arsenic concentrations in rhizosphere porewater must be greater than those in bulk soil porewater, because assuming arsenic concentrations to be the same in rhizosphere and bulk porewater indicated a discrepancy between arsenic intake through transpiration flux, and fern arsenic content. Processes other than mass flow of soluble arsenic from bulk soil to roots must be important for arsenic uptake (Barber, 1995).

If nutrients availability in soil is lower than *P. vittata* demand, *P. vittata* could employ nutrient-scavenging processes that release iron, phosphorus, and therefore arsenic from soil into porewater in the rhizosphere (Gerke, 2015; Meharg and Hartley-Whitaker, 2002), increasing porewater arsenic concentrations locally to potentially very high concentrations. We suggest that the majority of the arsenic taken up into *P. vittata* was mobilized directly in the rhizosphere, similarly to others who found greater desorption of cadmium in cadmium hyperaccumulator rhizospheric compared to bulk soils (Ingwersen et al., 2006).

We hypothesize that higher diffusivity due to greater connected pore space in the medium-textured soil could lead to transport of the arsenic released in the rhizosphere to the bulk soil, where it is then available for leaching. Similarly, rhizosphere DOC could be transported to the bulk soil and promote release of arsenic. However, in the coarse-textured soil characterized by lower porosity, larger pores, lower saturated fraction, and predominantly advective flow, arsenic and DOC released in the rhizosphere did not contribute to bulk leachate arsenic concentrations and, conversely, arsenic in the bulk porewater was not as accessible to the plants.

4.5. Mechanisms of arsenic release from soil

We suggest rhizosphere arsenic mobilization is a byproduct of nutrient-scavenging processes, particularly iron-scavenging in the medium-textured soil, where we found higher iron concentrations in ferns and in root zone (near-surface) porewater. Specifically, arsenic release from soil could be coupled to phosphorus and iron release from soil iron oxide minerals (Lombi et al., 2000; Manning and Goldberg, 1996; Redman et al., 2002). Release processes could include ion exchange, ligand-enhanced dissolution, and reductive dissolution (Fitz et al., 2003; Gerke, 2015; Li et al., 2007; Marschner, 2011), likely tied to release of root exudates from *P. vittata* roots (Liu et al., 2016; Silva Gonzaga et al., 2006). We found primarily oxidized arsenic in our well-drained rhizosphere soil, suggesting processes including ion exchange and ligand-enhanced dissolution, likely coupled to rhizosphere DOC, are more important than reductive dissolution, similarly to in the Pine rhizosphere (Tappero et al., 2021).

Alternately, the predominance of oxidized species could indicate *P. vittata* preferentially took up reduced species, leaving oxidized species behind. We found evidence of reductive processes in the rhizosphere, with up to 41% of the arsenic present as arsenic(III) in rhizosphere soil, up to 100% of the arsenic present as arsenic(III) on and within roots, and iron(II) phases in rhizosphere soil, suggesting reduced arsenic and iron could play a secondary role in arsenic release and uptake. A high fraction of surficial arsenic(III) could indicate transport of arsenic toward the root and accumulation in the rhizoplane, with slower uptake of arsenic(III) (Wang et al., 2002) enriching arsenic(III) relative to arsenic(V) on the root surface. The presence of arsenic(III) on the root surface could also indicate efflux of arsenic(III) from roots, which has been proposed to be a secondary tolerance mechanism in *P. vittata* and other plants under arsenic stress (Chen et al., 2016; Wagner et al., 2020).

In bulk porewater, bulk soils, and soil aggregates, the predominance of arsenic(V) indicates arsenic can leach under oxic conditions. Arsenic availability for leaching, whether due to soil characteristics or influence of plant growth, is not dependent on reducing conditions. Indeed, arsenic (V) mobility in soil increases at the circumneutral to alkaline porewater pH we observed (Dixit and Hering, 2003). Arsenic mobilized as arsenic (III) could be oxidized, perhaps coupled to reduction (Amirbahman et al., 2006) of the moderately-available soil manganese. Leaching of root-derived dissolved organic carbon (Uselman et al., 2007; Vinther et al., 2005) could also increase arsenic release from bulk soil for leaching.

4.6. Arsenic release coupled to nutrient scavenging

Rhizosphere nutrient acquisition processes have a specific significance in the case of hyperaccumulators. Infertile soils could characterize the hyperaccumulator ecological niche (Koide et al., 1988), such that *P. vittata* employs scavenging techniques and associates with indigenous AMF to acquire necessary phosphorus and other nutrients. We found *Glomus* spp. including *F. mosseae* were present across all treatments whether due to colonization by indigenous mycorrhiza or due to inoculation.

In the very low nutrient coarse-textured soil, we hypothesize that extensive use of these scavenging processes cost metabolic energy, locally increased already high arsenic availability, led to high uptake of arsenic and consequently even more energy expenditure to sequester this arsenic, and ultimately resulted in low biomass containing arsenic at high concentrations. The lack of effect of supplemental phosphorus in the coarse-textured soil suggests it is a balance of phosphorus and other nutrients which are required to meet *P. vittata* nutritional needs.

In contrast, in the medium-textured soil, we hypothesize the ferns used less energy to acquire nutrients. Iron scavenging here was successful, apparently meeting fern nutrient needs and therefore limiting “byproduct” arsenic released from soil. Hence, *P. vittata* growing in the medium-textured soil experienced lower metabolic costs and consequently higher biomass until drought stress limited biomass production.

In keeping with evolution under phosphorus starvation conditions (Audet, 2013), our results suggest *P. vittata* is less tolerant to extractable phosphorus concentrations greater than that of the medium-textured soil (8.07 mg/kg). Fronds of *P. vittata* growing in its native habitat in China were only 0.08% phosphorus, and ferns including *P. vittata* had the lowest phosphorus content of any flora group in China (Han et al., 2005). We found phosphorus application delayed fern growth in both medium- and coarse-textured soils, as has been shown for tropical forest ferns (Walker et al., 1996), leading to smaller senescent fronds containing lower amounts of arsenic.

4.7. Significance of leaching

Our findings suggest that *P. vittata* is a good choice for remediation at the mesoscale, because arsenic uptake in ferns exceeded cumulative loss by leaching by an order of magnitude, and transpiration limited leaching compared to the absence of ferns. Decreased effluent volumes and cumulative arsenic leaching in both soils in the presence of ferns confirms the critical role transpiration plays in limiting water percolation and leaching of soluble, plant available constituents (Benjamin et al., 1996; Medalie et al., 1984).

The leaching to uptake ratio measured in this mesocosm system is not directly scalable to field conditions. We demonstrate that arsenic leaching during phytoextraction depends on soil characteristics, fern growth, and water input/evapotranspiration ratios, and therefore must be measured at the field scale. The constant water application required in our column study design could have increased leaching of arsenic relative to field applications. On the other hand, our experimental design could have limited plant growth and therefore nutrient scavenging activities, which we showed can increase arsenic release from soil. Larger biomass under field conditions could increase the influence of the nutrient scavenging geochemical processes observed here and lead to increases in arsenic mobilization for both uptake and potential leaching, explaining the excess loss of arsenic from soil observed under field conditions (Kertulis-Tartar et al., 2006; Matzen et al., 2020; Niazi et al., 2012).

Counterintuitively, because we showed that *P. vittata* continued to phytoextract arsenic under drought conditions from the medium-textured soil to effectively limit arsenic leaching, phytoextraction could be best suited for dry soils with lower arsenic availability. Here, even though frond arsenic concentrations were an order of magnitude greater in coarse-textured soil ferns, mass of accumulated arsenic in coarse-textured soil ferns was only 1.2 to 2.4 times that of medium-textured soil ferns, while leached arsenic was also greater in coarse-textured soil, due to the lower biomass and lower transpiration. Alternatively, phytostabilization (Bolan et al., 2011) with species with high transpiration rates but lower iron demand could limit biotic and abiotic arsenic leaching.

5. Conclusion

Our findings suggest a biogeochemical domino effect where fern-scale impacts ecosystem-scale arsenic cycling to potentially impact other ecological receptors. High arsenic accumulation in *P. vittata* comes with an ecological tradeoff, and the system price of the tradeoff depends on ability of lower soil horizons to sorb arsenic leached during *P. vittata* growth. High phytoavailable arsenic coupled with low nutrient content led to lower *P. vittata* biomass, likely a response to the higher metabolic cost of arsenic hyperaccumulation and unsuccessful nutrient scavenging. This led to greater arsenic leaching compared to in the soil with lower arsenic phytoavailability and higher nutrient content, where fern growth was greater such that transpiration curtailed leaching. However, this successful nutrient scavenging increased arsenic release and leaching relative to the absence of plant growth. In assessing *P. vittata* arsenic uptake, whether in phytoextraction-based agroecosystems or in naturally occurring populations in arsenic-enriched soil, attention should also be paid to downward mobility of arsenic, to minimize ecosystem harm.

CRediT authorship contribution statement

S.L. Matzen: Conceptualization, Data curation, Formal analysis, Funding acquisition, Investigation, Methodology, Project administration, Software, Supervision, Visualization, Writing – original draft, Writing –

review & editing. **G.P. Lobo:** Data curation, Formal analysis, Investigation, Methodology, Software, Visualization, Writing – original draft, Writing – review & editing. **S.C. Fakra:** Data curation, Formal analysis, Investigation, Methodology, Resources, Software, Supervision, Visualization, Writing – review & editing. **A. Kakouridis:** Data curation, Investigation, Methodology, Software, Visualization, Writing – original draft, Writing – review & editing. **P.S. Nico:** Conceptualization, Methodology, Writing – review & editing. **C.E. Pallud:** Conceptualization, Data curation, Formal analysis, Funding acquisition, Investigation, Methodology, Project administration, Resources, Supervision, Visualization, Writing – review & editing.

Declaration of competing interest

The authors declare that they have no known competing financial interests or personal relationships that could have appeared to influence the work reported in this paper.

Acknowledgements

We acknowledge that UC Berkeley and soils used in this research are part of the ancestral and unceded land of the Chochenyo speaking Ohlone people, land currently home to Muwekma Ohlone people. We benefited from use of this land and owe a debt to the Ohlone people.

We thank all undergraduate research interns at UC Berkeley.

This work was supported by the National Science Foundation Graduate Research Fellowship Program (under Grant No. DGE 1106400), the Research Institute for Humanity and Nature (Kyoto, Japan), the USDA National Institute of Food and Agriculture (HATCH project 1016950), Phipps Conservatory, the Clay Minerals Society, and the Berkeley Collegium, UC Berkeley. The funding sources had no involvement in study design; collection, analysis, and interpretation of data; the writing of the manuscript; nor the decision to publish the findings.

This research used resources of the Advanced Light Source, which is a DOE Office of Science User Facility under contract no. DE-AC02-05CH11231. Use of the Stanford Synchrotron Radiation Lightsource (SSRL), SLAC National Accelerator Laboratory, is supported by the U.S. Department of Energy, Office of Science, Office of Basic Energy Sciences under Contract No. DE-AC02-76SF00515. We thank Erik Nelson for his support at SSRL.

Appendix A. Supplementary data

Supplementary data to this article can be found online at https://doi.org/10.1016/j.scitotenv.2021.151803.

References

Alford, E.R., Pilon-Smits, E.A.H., Paschke, M.W., 2010. Metallophytes-a view from the rhizosphere. Plant Soil 337, 33–50.

Amirbahman, A., Kent, D.B., Curtis, G.P., Davis, J.A., 2006. Kinetics of sorption and abiotic oxidation of arsenic(III) by aquifer materials. Geochim. Cosmochim. Acta 70, 533–547.

Arai, Y., Dahle, J.T., 2018. Redox-ligand complexation controlled chemical fate of ceria nanoparticles in an agricultural soil. J. Agric. Food Chem. 66, 6646–6653.

Audet, P., 2013. Examining the ecological paradox of the 'mycorrhizal-metal-hyperaccumulators'. Arch. Agron. Soil Sci. 59, 549–558.

Baker, A.J.M., Whiting, S.N., 2002. In search of the holy grail - a further step in understanding metal hyperaccumulation? New Phytol. 155, 1–4.

Barber, S.A., 1995. Soil Nutrient Bioavailability: A Mechanistic Approach. 2nd ed. John Wiley and Sons Inc, New York.

Barton, K., 2019. MuMIn: Multi-model Inferance, Version 1.43.17 ed.

Beesley, L., Moreno-Jimenez, E., Clemente, R., Lepp, N., Dickinson, N., 2010. Mobility of arsenic, cadmium and zinc in a multi-element contaminated soil profile assessed by *in-situ* soil pore water sampling, column leaching and sequential extraction. Environ. Pollut. 158, 155–160.

Benjamin, J.G., Ahuja, L.R., Allmaras, R.R., 1996. Modelling corn rooting patterns and their effects on water uptake and nitrate leaching. Plant Soil 179, 223–232.

Bolan, N.S., Park, J.H., Robinson, B., Naidu, R., Huh, K.Y., 2011. Phytostabilization: a green approach to contaminant containment. In: Sparks, D.L. (Ed.), Advances in Agronomy. 112. Elsevier, pp. 145–204.

Bolyen, E., Rideout, J.R., Dillon, M.R., Bokulich, N.A., Abnet, C.C., Al-Ghalith, G.A., Caporaso, J.G., 2019. Reproducible, interactive, scalable and extensible microbiome data science using QIIME 2. Nat. Biotechnol. 37, 852–857.

Brodie, E.L., Joyner, D.C., Faybishenko, B., Conrad, M.E., Rios-Velazquez, C., Malave, J., Hazen, T.C., 2011. Microbial community response to addition of polylactate compounds to stimulate hexavalent chromium reduction in groundwater. Chemosphere 85, 660–665.

Caille, N., Swanwick, S., Zhao, F.J., McGrath, S.P., 2004. Arsenic hyperaccumulation by *Pteris vittata* from arsenic contaminated soils and the effect of liming and phosphate fertilisation. Environ. Pollut. 132, 113–120.

Callahan, B.J., McMurdie, P.J., Rosen, M.J., Han, A.W., Johnson, A.J., Holmes, S.P., 2016. DADA2: high-resolution sample inference from Illumina amplicon data. Nat. Methods 13, 581–583.

Cao, X., Ma, L.Q., Shiralipour, A., 2003. Effects of compost and phosphate amendments on arsenic mobility in soils and arsenic uptake by the hyperaccumulator, *Pteris vittata* L. Environ. Pollut. 126, 157–167.

Chaney, R.L., Angle, J.S., Broadhurst, C.L., Peters, C.A., Tappero, R.V., Sparks, D.L., 2007. Improved understanding of hyperaccumulation yields commercial phytoextraction and phytomining technologies. J. Environ. Qual. 36, 1429–1443.

Chen, T.-B., Wei, C., Huang, Z., Huang, Q., Lu, Q., Fan, Z., 2002. Effect of phosphorus on arsenic accumulation in As-hyperaccumulator *Pteris vittata* L. and its implication. Chin. Sci. Bull. 47, 902–905.

Chen, Y., Fu, J.W., Han, Y.H., Rathinasabapathi, B., Ma, L.Q., 2016. High As exposure induced substantial arsenite efflux in As-hyperaccumulator *Pteris vittata*. Chemosphere 144, 2189–2194.

Ciurli, A., Lenzi, L., Alpi, A., Pardossi, A., 2014. Arsenic uptake and translocation by plants in pot and field experiments. Int. J. Phytoremediation 16, 804–823.

Danh, L.T., Truong, P., Mammucari, R., Foster, N., 2014. A critical review of the arsenic uptake mechanisms and phytoremediation potential of *Pteris vittata*. Int. J. Phytoremediation 16, 429–453.

Dixit, S., Hering, J.G., 2003. Comparison of arsenic(V) and arsenic(III) sorption onto iron oxide minerals: implications for arsenic mobility. Environ. Sci. Technol. 37, 4182–4189.

Dumbrell, A.J., Ashton, P.D., Aziz, N., Feng, G., Nelson, M., Dytham, C., Helgason, T., 2011. Distinct seasonal assemblages of arbuscular mycorrhizal fungi revealed by massively parallel pyrosequencing. New Phytol 190, 794–804.

Egan, C.P., Rummel, A., Kokkoris, V., Klironomos, J., Lekberg, Y., Hart, M., 2018. Using mock communities of arbuscular mycorrhizal fungi to evaluate fidelity associated with Illumina sequencing. Fungal Ecol. 33, 52–64.

van der Ent, A., Baker, A.J.M., Reeves, R.D., Pollard, A.J., Schat, H., 2013. Hyperaccumulators of metal and metalloid trace elements: facts and fiction. Plant Soil 362, 319–334.

Fayiga, A.O., Ma, L.Q., 2006. Using phosphate rock to immobilize metals in soil and increase arsenic uptake by hyperaccumulator *Pteris vittata*. Sci. Total Environ. 359, 17–25.

Fayiga, A.O., Saha, U.K., 2016. Arsenic hyperaccumulating fern: implications for remediation of arsenic contaminated soils. Geoderma 284, 132–143.

Fitz, W.J., Wenzel, W.W., Zhang, H., Nurmi, J., Stipek, K., Fischerova, Z., Stingeder, G., 2003. Rhizosphere characteristics of the arsenic hyperaccumulator *Pteris vittata* L. and monitoring of phytoremoval efficiency. Environ. Sci. Technol. 37, 5008–5014.

Foster, H.L., 1981. The basic factors which determine inherent soil fertility in Uganda. J. Soil Sci. 32, 12.

Gaudet, J.P., Jégat, H., Vachaud, G., Wierenga, P.J., 1977. Solute transfer, with exchange between mobile and stagnant water, through unsaturated sand. Soil Sci. Soc. Am. J. 41, 665–671.

Gee, G., Or, D., 2002. Particle-size analysis. In: Dane, J.H., Topp, G.C. (Eds.), Methods of Soil Analysis: Part 4 Physical Methods. Soil Science Society of America, Madison, WI, pp. 255–293.

Gerke, J., 2015. The acquisition of phosphate by higher plants: effect of carboxylate release by the roots. A critical review. J. Plant Nutr. Soil Sci. 178, 351–364.

Grossman, R.B., Reinsch, T.G., 2002. Bulk density and linear extensibility. In: Dane, J.H., Topp, G.C. (Eds.), Methods of Soil Analysis: Part 4 Physical Methods. Soil Science Society of America, Madison, WI, pp. 201–228.

Hale, J.R., Foos, A., Zubrow, J.S., Cook, J., 2008. Better characterization of arsenic and chromium in soils: a field-scale example. J. Soil Contam. 6, 371–389.

Han, W., Fang, J., Guo, D., Zhang, Y., 2005. Leaf nitrogen and phosphorus stoichiometry across 753 terrestrial plant species in China. New Phytol. 168, 377–385.

Holzbecher, E., 2012. Environmental Modeling Using MATLAB. Second ed. Springer-Verlag, Berlin Heidelberg.

Ingwersen, J., Bucherl, B., Neumann, G., Streck, T., 2006. Cadmium leaching from microlysimeters planted with the hyperaccumulator *Thlaspi caerulescens*: experimental findings and modeling. J. Environ. Qual. 35, 2055–2065.

Jacobs, L.W., Keeney, D.R., 2008. Arsenic - phosphorus interactions on corn. Commun. Soil Sci. Plant Anal. 1, 85–93.

Karandashov, V., Bucher, M., 2005. Symbiotic phosphate transport in arbuscular mycorrhizas. Trends Plant Sci. 10, 22–29.

Kertulis-Tartar, G.M., Ma, L.Q., Tu, C., Chirenje, T., 2006. Phytoremediation of an arsenic-contaminated site using *Pteris vittata* L.: a two-year study. Int. J. Phytoremediation 8, 311–322.

Kidd, P., Barcelo, J., Bernal, M.P., Navari-Izzo, F., Poschenrieder, C., Shilev, S., Monterroso, C., 2009. Trace element behaviour at the root-soil interface: implications in phytoremediation. Environ. Exp. Bot. 67, 243–259.

Koide, R.T., Huenneke, L.F., Hamburg, S.P., Mooney, H.A., 1988. Effects of applications of fungicide, phosphorus and nitrogen on the structure and productivity of an annual serpentine plant community. Funct. Ecol. 2, 335–344.

Kopittke, P.M., Wang, P., Lombi, E., Donner, E., 2017. Synchrotron-based X-ray approaches for examining toxic trace metal(loid)s in soil-plant systems. J. Environ. Qual. 46, 1175–1189.

Lee, J., Lee, S., Young, J.P., 2008. Improved PCR primers for the detection and identification of arbuscular mycorrhizal fungi. FEMS Microbiol. Ecol. 65, 339–349.

Lessl, J.T., Ma, L.Q., 2013. Sparingly-soluble phosphate rock induced significant plant growth and arsenic uptake by *Pteris vittata* from three contaminated soils. Environ. Sci. Technol. 47, 5311–5318.

Leung, H.M., Ye, Z.H., Wong, M.H., 2006. Interactions of mycorrhizal fungi with *Pteris vittata* (As hyperaccumulator) in As-contaminated soils. Environ. Pollut. 139, 1–8.

Li, L., Li, S.M., Sun, J.H., Zhou, L.L., Bao, X.G., Zhang, H.G., Zhang, F.S., 2007. Diversity enhances agricultural productivity via rhizosphere phosphorus facilitation on phosphorus-deficient soils. Proc. Natl. Acad. Sci. U. S. A. 104, 11192–11196.

Li, J.T., Gurajala, H.K., Wu, L.H., van der Ent, A., Qiu, R.L., Baker, A.J.M., Shu, W.S., 2018. Hyperaccumulator plants from China: a synthesis of the current state of knowledge. Environ. Sci. Technol. 52, 11980–11994.

Liao, X.-Y., Chen, T.-B., Lei, M., Huang, Z.-C., Xiao, X.-Y., An, Z.-Z., 2004. Root distributions and elemental accumulations of *Pteris vittata* from As-contaminated soils. Plant Soil 261, 109–116.

Liu, Y., Zhu, Y.G., Chen, B.D., Christie, P., Li, X.L., 2005. Influence of the arbuscular mycorrhizal fungus *Glomus mosseae* on uptake of arsenate by the As hyperaccumulator fern *Pteris vittata* L. Mycorrhiza 15, 187–192.

Liu, X., Fu, J.W., Guan, D.X., Cao, Y., Luo, J., Rathinasabapathi, B., Ma, L.Q., 2016. Arsenic induced phytate exudation, and promoted $FeAsO_4$ dissolution and plant growth in As-hyperaccumulator *Pteris vittata*. Environ. Sci. Technol. 50, 9070–9077.

Lombi, E., Sletten, R.S., Wenzel, W.W., 2000. Sequentially extracted arsenic from different size fractions of contaminated soils. Water Air Soil Pollut. 124, 319–332.

Ma, L.Q., Komar, K.M., Tu, C., Zhang, W.H., Cai, Y., Kennelley, E.D., 2001. A fern that hyperaccumulates arsenic - a hardy, versatile, fast-growing plant helps to remove arsenic from contaminated soils. Nature 409, 579.

Maestri, E., Marmiroli, M., Visioli, G., Marmiroli, N., 2010. Metal tolerance and hyperaccumulation: costs and trade-offs between traits and environment. Environ. Exp. Bot. 68, 1–13.

Manning, B.A., Goldberg, S., 1996. Modeling competitive adsorption of arsenate with phosphate and molybdate on oxide minerals. Soil Sci. Soc. Am. J. 60, 121–131.

Marcus, M.A., MacDowell, A.A., Celestre, R., Manceau, A., Miller, T., Padmore, H.A., Sublett, R.E., 2004. Beamline 10.3.2 at ALS: a hard X-ray microprobe for environmental and materials sciences. J. Synchrotron. Radiat. 11, 239–247.

Marschner, H., 2011. Mineral Nutrition of Higher Plants. Academic Press.

Marschner, H., Romheld, V., 1994. Strategies of plants for acquisition of iron. Plant Soil 165, 261–274.

Masscheleyn, P.H., Delauna, R.D., Patrick, J., William, H., 1991. Effect of redox potential and pH on arsenic speciation and solubility in a contaminated soil. Environ. Sci. Technol. 25, 1414–1419.

Matzen, S., Fakra, S., Nico, P., Pallud, C., 2020. *Pteris vittata* arsenic accumulation only partially explains soil arsenic depletion during field-scale phytoextraction. Soil Syst. 4.

Medalie, L., Bowden, W.B., Smith, C.T., 1984. Nutrient leaching following land application of aerobically digested municipal sewage sludge in a northern hardwood forest. J. Environ. Qual. 23, 130–138.

Meharg, A.A., Hartley-Whitaker, J., 2002. Arsenic uptake and metabolism in arsenic resistant and nonresistant plant species. New Phytol. 154, 29–43.

Niazi, N.K., Singh, B., Van Zwieten, L., Kachenko, A.G., 2012. Phytoremediation of an arsenic-contaminated site using *Pteris vittata* L. and *Pityrogramma calomelanos* var. austroamericana: a long-term study. Environ. Sci. Pollut. Res. 19, 3506–3515.

Oksanen, J., Blanchet, F.G., Friendly, M., Kindt, R., Legendre, P., McGlinn, D., … Wagner, H., 2020. Vegan: Community Ecology Package, 2.5-7 ed.

Öpik, M., Vanatoa, A., Vanatoa, E., Moora, M., Davison, J., Kalwij, J.M., Zobel, M., 2010. The online database Maarj*AM* reveals global and ecosystemic distribution patterns in arbuscular mycorrhizal fungi (Glomeromycota). New Phytol 188, 223–241.

Pallud, C., Dechesne, A., Gaudet, J.P., Debouzie, D., Grundmann, G.L., 2004. Modification of spatial distribution of 2,4-dichlorophenoxyacetic acid degrader microhabitats during growth in soil columns. Appl. Environ. Microbiol. 70, 2709–2716.

Pallud, C., Rhoades, C.C., Schneider, L., Dwivedi, P., Borch, T., 2020. Temperature-induced iron (III) reduction results in decreased dissolved organic carbon export in subalpine wetland soils, Colorado, USA. Geochim. Cosmochim. Acta 280, 148–160.

Poppe, L.J., Paskevich, V.F., Hathaway, J.C., Blackwood, D.S., 2002. A laboratory manual for X-ray powder diffraction. U. S. Geological Survey Open-File Report 01-041. U. S. Geological Survey, Woods Hole, MA, pp. 1–88.

R Core Team, 2020. R: A Language and Environment for Statistical Computing. R Foundation for Statistical Computing, Vienna, Austria.

Rascio, N., Navari-Izzo, F., 2011. Heavy metal hyperaccumulating plants: how and why do they do it? And what makes them so interesting? Plant Sci. 180, 169–181.

Redman, A.D., Macalady, D.L., Ahmann, D., 2002. Natural organic matter affects arsenic speciation and sorption onto hematite. Environ. Sci. Technol. 36, 2889–2896.

Reeves, R., 2006. Hyperaccumulation of trace elements by plants. In: Morel, J.L., Echevarria, G., Goncharova, N. (Eds.), Phytoremediation of Metal-contaminated Soils, pp. 25–52.

Roberts, L.C., Hug, S.J., Ruettimann, T., Billah, M., Khan, A.W., Rahman, M.T., 2004. Arsenic removal with iron(II) and iron(III) waters with high silicate and phosphate concentrations. Environ. Sci. Technol. 38, 307–315.

Saifullah, Meers, E., Qadir, M., de Caritat, P., Tack, F.M.G., Du Laing, G., Zia, M.H., 2009. EDTA-assisted Pb phytoextraction. Chemosphere 74, 1279–1291.

Shelmerdine, P.A., Black, C.R., McGrath, S.P., Young, S.D., 2009. Modelling phytoremediation by the hyperaccumulating fern, *Pteris vittata*, of soils historically contaminated with arsenic. Environ. Pollut. 157, 1589–1596.

Silva Gonzaga, M.I., Santos, J.A., Ma, L.Q., 2006. Arsenic chemistry in the rhizosphere of *Pteris vittata* L. and *Nephrolepis exaltata* L. Environ. Pollut. 143, 254–260.

da Silva, E.B., Lessl, J.T., Wilkie, A.C., Liu, X., Liu, Y., Ma, L.Q., 2018. Arsenic removal by As-hyperaccumulator *Pteris vittata* from two contaminated soils: a 5-year study. Chemosphere 206, 736–741.

Smith, E., Smith, J., Naidu, R., 2006. Distribution and nature of arsenic along former railway corridors of South Australia. Sci. Total Environ. 363, 175–182.

Tack, F.M.G., Meers, E., 2010. Assisted phytoextraction: helping plants to help us. Elements 6, 383–388.

Tappero, R., Liao, H.-L., Bhatnagar, J.M., Averill, C., Chen, K.-H., Zhang, K., Vilgalys, R., 2021. Non-reductive, Ligand-promoted Dissolution Is Responsible for Enhanced Weathering of Ferric (Oxy)hydroxides in the Pine (Mycor)rhizosphere, Goldschmidt, Lyon, France.

Trotta, A., Falaschi, P., Cornara, L., Minganti, V., Fusconi, A., Drava, G., Berta, G., 2006. Arbuscular mycorrhizae increase the arsenic translocation factor in the As hyperaccumulating fern *Pteris vittata* L. Chemosphere 65, 74–81.

Tu, S., Ma, L.Q., 2003. Interactive effects of pH, arsenic and phosphorus on uptake of As and P and growth of the arsenic hyperaccumulator *Pteris vittata* L. under hydroponic conditions. Environ. Exp. Bot. 50, 243–251.

United States Department of Agriculture, 2001. USDA NRCS Soil Quality Test Kit Guide.

Uselman, S.M., Qualls, R.G., Lilienfein, J., 2007. Contribution of root vs. leaf litter to dissolved organic carbon leaching through soil. Soil Sci. Soc. Am. J. 71, 1555–1563.

Vinther, F.P., Hansen, E.M., Eriksen, J., 2005. Leaching of soil organic carbon and nitrogen in sandy soils after cultivating grass-clover swards. Biol. Fertil. Soils 43, 12–19.

Wagner, S., Hoefer, C., Puschenreiter, M., Wenzel, W.W., Oburger, E., Hann, S., Santer, J., 2020. Arsenic redox transformations and cycling in the rhizosphere of *Pteris vittata* and *Pteris quadriaurita*. Environ. Exp. Bot 177, 104122–104133.

Walker, L.R., Zimmerman, J.K., Lodge, D.J., Guzman-Grajales, S., 1996. An altitudinal comparison of growth and species composition in hurricane- damaged forests in Puerto Rico. J. Ecol. 84, 877–889.

Wan, X.M., Lei, M., Chen, T.B., 2016. Cost-benefit calculation of phytoremediation technology for heavy-metal-contaminated soil. Sci. Total Environ. 563, 796–802.

Wang, J.R., Zhao, F.J., Meharg, A.A., Raab, A., Feldmann, J., McGrath, S.P., 2002. Mechanisms of arsenic hyperaccumulation in *Pteris vittata*. Uptake kinetics, interactions with phosphate, and arsenic speciation. Plant Physiol. 130, 1552–1561.

Wenzel, W.W., Unterbrunner, R., Sommer, P., Sacco, P., 2003. Chelate-assisted phytoextraction using canola (*Brassica napus* L.) in outdoors pot and lysimeter experiments. Plant Soil 249, 83–96.

Western Regional Climate Center, 2000. Berkeley, California (040693) Period of Record Monthly Climate Summary.

Whitehead, H.C., Feth, J.H., 1964. Chemical composition of rain, dry fallout, and bulk precipitation at Menlo Park, California, 1957–1959. J. Geophys. Res. 69, 3319–3333.

Wicke, D., Cochrane, T.A., O'Sullivan, A.D., Cave, S., Derksen, M., 2014. Effect of age and rainfall pH on contaminant yields from metal roofs. Water Sci. Technol. 69, 2166–2173.

Woolson, E.A., Axley, J.H., Kearne, P.C., 1973. The chemistry and phytotoxicity of arsenic in soils - II. Effects of time and phosphorus. Soil Sci. Soc. Am. Proc. 37, 254–259.

Wu, F.Y., Ye, Z.H., Wu, S.C., Wong, M.H., 2007. Metal accumulation and arbuscular mycorrhizal status in metallicolous and nonmetallicolous populations of *Pteris vittata* L. and *Sedum alfredii* Hance. Planta 226, 1363–1378.

Wu, Z., Banuelos, G.S., Lin, Z.Q., Liu, Y., Yuan, L., Yin, X., Li, M., 2015. Biofortification and phytoremediation of selenium in China. Front. Plant Sci. 6, 136.

Xie, Q.E., Yan, X.L., Liao, X.Y., Li, X., 2009. The arsenic hyperaccumulator fern *Pteris vittata* L. Environ. Sci. Technol. 43, 8488–8495.

Xu, W., Kachenko, A.G., Singh, B., 2010. Effect of soil properties on arsenic hyperaccumulation in *Pteris vittata* and *Pityrogramma calomelanos* var. austroamericana. Int. J. Phytoremediation 12, 174–187.

Yang, Q., Tu, S., Wang, G., Liao, X., Yan, X., 2012. Effectiveness of applying arsenate reducing bacteria to enhance arsenic removal from polluted soils by *Pteris vittata* L. Int. J. Phytoremediation 14, 89–99.

Yang, J., Guo, Y., Yan, Y., Yang, J., Wan, X., Guo, J., Lei, M., 2019. Phytoaccumulation of As by *Pteris vittata* supplied with phosphorus fertilizers under different soil moisture regimes – a field case. Ecol. Eng. 138, 274–280.

Zhang, H., Selim, H.M., 2006. Modeling the transport and retention of arsenic (V) in soils. Soil Sci. Soc. Am. J. 70, 1677–1687.